Introduction of a Breakage Probability Function in the Hydrocracking Reactor Model

Simone Gamba,[†] Laura A. Pellegrini,*[,†] Vincenzo Calemma,[‡] and Chiara Gambaro[‡]

Dipartimento di Chimica, Materiali e Ingegneria Chimica "G. Natta", Politecnico di Milano, Piazza Leonardo da Vinci 32, I-20133 Milano, Italy, and Eni S.p.A., Divisione Refining & Marketing — Centro Ricerche di San Donato Milanese, Via Felice Maritano 26, I-20097 San Donato Milanese, Milano, Italy

This paper shows how a breakage probability function for the C−C bonds, elaborated from experimental evidence reported in literature, is introduced in the reactor model for the hydrocracking of Fischer−Tropsch waxes. The results demonstrate a better response to the variation of the operating conditions (especially as concerns temperature) and show product distributions closer to the experimental ones than those predicted by the previous model [Pellegrini, L. A. et al. *Chem. Eng. Sci.* **2008**, *63*, 4285]. The agreement with the experimental data has also been enhanced introducing a dependence on temperature (in addition to the dependence on the number of carbon atoms) in the expressions for the Langmuir constants and giving the equilibrium constants for isomerization reactions a new function derived from a thermodynamic study.

1. Introduction

It is well-known that the Fischer−Tropsch (FT) synthesis leads to the formation of products essentially made up of *n*-paraffins (>90%), along with smaller percentages of oxygenated compounds and olefins. The FT products are characterized by a wide range of molecular weights, ranging from C_1 to C_{80} and higher, and the current cobalt catalyzed, low temperature, slurry FT technologies give product distributions strongly shifted toward long chain paraffins.[1] As a consequence, the yields in middle distillates (MD; i.e., the 150−370 °C cut) are rather limited, and moreover, MD show very poor cold flow properties (i.e., relatively high melting point) that hamper their use as transportation fuel. In spite of the efforts, the improvement of the intrinsic selectivity of the FT synthesis toward desired fractions (i.e., MD) has met with limited success and therefore the FT products need to undergo an upgrading process to improve both yields and quality of middle distillates.

It is generally accepted that the most effective route to maximize the overall MD yield is to subject the FT waxes to a hydrocracking step.[2−4] During the hydroconversion over a bifunctional catalyst,[5−7] the cracking of long chain alkanes leads to the increase of middle distillate fraction (MD yields range between 80 and 85%)[8] while the isomerization remarkably improves MD cold flow properties.[9] Thus, catalytic hydrocracking has been the subject of numerous investigations.[10−18]

Specifically concerning the modeling of the hydrocracking process, a kinetic model at the mechanistic level has been proposed in literature.[19] Although the mechanistic approach is a promising methodology to model the hydroconversion of hydrocarbons in terms of fundamental reaction steps, it is hardly applicable to complex mixtures like FT waxes owing to the huge number of elementary steps involved (e.g., *n*-C_{16} hydrocracking modeling requires a scheme containing 465 species and 1503 reactions)[19] and the consequent calculation power required: in that case, a pathway-level kinetic model[19] based on Langmuir−Hinshelwood−Hougen−Watson kinetic equations can be a suitable approach.

Moreover during the hydrocracking process of *n*-paraffin mixtures characterized by a wide range of molecular weights, there is the contemporaneous presence of gas−liquid−solid phases. A possible method to address the problem of a three-phase hydrocracking is the use of the fugacity instead of the partial pressure of compounds. Such an approach has led to promising results in modeling the hydroconversion of FT waxes.[20]

This paper concerns the modeling of the catalytic hydrocracking of FT waxes (a mixture of C_5−C_{70} *n*-paraffins) over a bifunctional catalyst (platinum supported on amorphous silica−alumina) in the following range of operating conditions of industrial interest: temperature 616.15−648.15 K; pressure 35−60 bar; H_2/waxes ratio 0.06−0.15 kg/kg; weight hourly space velocity (WHSV) 1−3 $kg_{n\text{-}C_{in}}/(kg_{cat}\cdot h)$. The details about the experimental plan, materials, and methods of analysis have already been reported.[20,21]

The results have been obtained with a kinetic model in which some simplifying hypotheses of a previous model,[20] concerning the rupture of C−C bonds, have been removed. Particularly, in this case, there is a basic assumption of a probability distribution for the rupture of C−C bonds in a given aliphatic similar to that obtained with model compounds in ideal hydrocracking conditions.

2. Literature on Hydrocracking: Product Distribution

A review of literature on experimental evidence for hydrocracking has been the starting point for developing the model.

A general remark regarding thermal vs catalytic cracking (which present quite different characteristics)[22] confirms the type of products obtained in our hydrocracking experiments: in the case of thermal cracking, the main products are ethylene and *n*-α-olefins with non-negligible quantities of methane and ethane and little quantities of branched aliphatics. In the case of catalytic cracking, the products are negligible quantities of methane, ethane, ethylene, and *n*-α-olefins and a great amount of branched aliphatics.[23]

For catalytic cracking, Martens et al.[18] report a number of data from experiments on catalysts constituted of nonstructured zeolites charged with 0.5−1.0% Pt; the most significant points are the following: (a) high selectivity toward the isomers of

* To whom correspondence should be addressed. Tel.: +39 02 2399 3237. Fax: +39 02 7063 8173. E-mail: laura.pellegrini@polimi.it.
[†] Politecnico di Milano.
[‡] Centro Ricerche di San Donato Milanese.

10.1021/ie8019455 CCC: $40.75
Published on Web 04/30/2009

the inlet hydrocarbons for medium-low conversions, which shows that the first step of hydrocracking is isomerization; (b) the primary cracking leads to a symmetric distribution in the number of carbon atoms for the products; (c) for the reaction of n-C_{15} and n-C_{17} on Pt/US, the secondary cracking is significant for conversions higher than 65%; (d) there is a high yield in monobranched compounds; (e) the distribution of the products coming from the cracking of n-C_8, isooctane, n-C_{10}, and n-C_{12} is a function of the conversion alone and is not dependent on pressure and temperature; (f) there is no production of methane and ethane, while small quantities of propane are formed.

According to Sie,[24] the paraffin with the lowest number of carbon atoms that can give cracking products with the above-reported distribution is C_7. This assumption is supported by other authors' experimental evidence. Sie[25] reports unpublished experimental works by Kouwenhoven (1967) and Wagstaff (1972) which show that, with a feed stream of n-C_5 and n-C_6 on Pt/mordenite, it is possible to obtain a selectivity toward isomerization of 100%, while with a feed of n-C_7 the selectivity is reduced to 30%. Martens et al.[18] experiments on heptane cracking (conversion 39% at 475 K and 1 atm) gave rise to equimolar quantities of C_3 and iso-C_4.

From the preceding analysis, the following conclusions, that constitute the bases for the hydrocracking modeling, can be drawn: (a) n-C_4 does not isomerize; (b) iso-C_4 does not crack; (c) n-C_5 can isomerize but iso-C_5 does not crack; (d) n-C_7 cracks giving rise, in equimolar quantities, to C_3 and iso-C_4.

To obtain lower carbon number products (i.e., C_1 and C_2) from cracking, more severe conditions must be applied; for instance, hexane can crack under severe conditions (temperature: 723 K) giving non-negligible quantities of methane and ethane (hydrogen can be produced too, at higher hydrocarbon partial pressure) and a low ratio of iso-butane/n-butane.[26] In our case however, methane and ethane are present in the product stream and their amount is not negligible. This is probably due to the direct hydrogenolisis of the n-paraffins because of the metallic function of the Pt catalyst, though it seems that the amount of products according to this mechanism is not important.[19]

For this reason, at this point, the production of methane and ethane has been assumed to derive from the cracking of C_6, whose bonds break all approximately with the same probability. The C_4 derived from the cracking of C_6 is linear.

3. Probability of Cracking

Carbon number distribution in the products obtained by hydrocracking of n-paraffins has been the subject of a significant amount of research.

Weitkamp[27,28] experimentally determined the carbon number spectra of the products obtained by primary hydrocracking of n-alkanes from n-heptane to n-hexadecane over a Pt/Ca/Y zeolite catalyst, while Schulz and Weitkamp[15] reported on the carbon number distribution in products from hydrocracking of n-dodecane on other types of zeolitic catalysts.

In general, these experiments over zeolitic catalysts show a common behavior: a virtual absence of C_1, C_2, and C_{n_C-1}, C_{n_C-2}, while the other hydrocarbon fragments are present in about the same molar amount with the exception of C_3 and C_{n_C-3}, whose production is somewhat less than half of that of the intermediate fragments.[25]

This feature is also common to a series of experiments over nonzeolitic catalysts: hydrocracking of C_{20},[29] n-hexadecane,[30,31] and hydrocracking of FT waxes.[32]

Table 1. Comparison between Experimental Results of Cracking Tests by Martens et al.[18] and Data (Indicated with *) Calculated with the *A* Probability of Cracking

cracked paraffin	product percentage									
	C_3	C_3*	C_4	C_4*	C_5	C_5*	C_6	C_6*	C_7	C_7*
n-C_8	20.5	25.0	59.0	50.0	20.5	25.0	0.0	0.0	0.0	0.0
n-C_9	9.0	16.7	41.3	33.3	40.8	33.3	9.0	16.7	0.0	0.0
n-C_{10}	5.0	12.5	28.5	25.0	33.0	25.0	28.5	25.0	5.0	12.5

Table 2. Percentages on the Total of the Linear Products without C_3 and C_{n_C-3}

cracked paraffin	%
n-C_8	22.0
n-C_9	17.6
n-C_{10}	12.8

So, the cracking product distribution (paraffins with $n_C \geq 8$) from linear chains can be based on the following simplifying remarks:[25] (a) all the products between C_4 and C_{n_C-4} form in equimolar quantities; (b) the quantity of fragments C_3 and C_{n_C-3} is equal to half of the quantity of each fragment between C_4 and C_{n_C-4}; (c) methane and ethane are not formed.

In a paraffin with n_C carbon atoms (for $n_C \geq 8$), there are $n_C - 1$ bonds, and consequently, with the exception of the six terminal bonds, $n_C - 7$ bonds which break with the same probability; there are four bonds that present no probability of cracking (they are the four terminal bonds that would give rise to C_1, C_2, C_{n_C-1}, C_{n_C-2}); there are two bonds (those from whose cracking C_3 and C_{n_C-3} derive) that break with a probability equal to half of the cracking probability of the other $n_C - 7$.

Let us assume that A represents the cracking probability of the $n_C - 7$ bonds. $A/2$ is the cracking probability of the third bond and of the $(n_C - 3)$th bond.

We can write

$$(n_C - 7)A + 2A/2 = 1 \tag{1}$$

and derive the value of cracking probability A:

$$A = \frac{1}{n_C - 6} \tag{2}$$

So, starting from n-octane, paraffins will break giving rise to $2An^0$ moles of each product between C_4 and C_{n_C-4} and to $2(A/2)n^0 = An^0$ moles of C_3 and C_{n_C-3}, where n^0 is the initial value of the paraffin moles.

Martens et al.[18] report the experimental results of cracking tests of n-heptane to n-decane over a Pt/USY catalyst. Experimental data (clearly related to a primary cracking since product distributions are symmetric) can be worked out and compared with the ones calculated according to the probability of cracking A derived previously; the results are reported in Table 1.

It can be seen that the probability of cracking assigned to the third and the $(n_C - 3)$th bonds gives more C_3 and C_{n_C-3} products than those obtained experimentally. Consequently the products belonging to the range C_4 and C_{n_C-4} are underestimated but the proposed product distribution can be considered reliable. Furthermore from experimental data,[18] it can be inferred that C_{n_C-3} fragments formed are practically totally branched. Instead, as Table 2 shows, there is a non-negligible amount of linear paraffins among the cracking products[18] with a carbon number from 4 to $n_C - 4$ (where n_C is the carbon number of the cracked paraffins). This quantity decreases when increasing the carbon number of the feed.

Thus in the modeling process, it will be necessary to take into account that cracking products can be either linear or branched.

4. Kinetic Modeling

The hydrocracking mechanism for temperatures lower than 693 K is essentially the carbenium ion chemistry of acid cracking coupled with the metal hydro/dehydrogenation function. The widely accepted mechanism includes the formation of an intermediate carbocation followed by the splitting of carbocation after rearrangement.

Several studies have concluded that the reaction mechanism for hydrocracking with zeolitic catalyst is similar to that for amorphous catalyst.[27,31]

The elementary steps used to model the mechanism of paraffin hydrocracking over a bifunctional catalyst can be summarized as follows: (1) dehydrogenation of *n*-paraffins to *n*-olefins on metallic sites; (2) protonation of olefins to carbenium ions on acidic sites; (3) carbenium ion hydride shift on acidic sites; (4) carbenium ion methyl shift on acidic sites; (5) protonated cyclopropane intermediate mediated branching of carbenium ion on acidic sites; (6) carbenium ion cracking through β-scission on acidic sites; (7) deprotonation of carbenium ions to olefins on acidic sites; (8) hydrogenation of olefins to paraffins on metallic sites.

The approach chosen for modeling the FT product hydrocracking reactor must act as a correct compromise between the complexity of a detailed molecular approach and the simple lump model.

Traditional models implemented lumped schemes, where hydrocarbons were aggregated into lumps characterized by global properties (NBP, average MW). These models are not flexible and are unable to handle a wide range of feeds.

On the hand, approaches that account for the fundamentals underlying hydrocracking reactions require a detailed molecular scheme and, therefore, may be too onerous when complex petroleum feedstocks (up to C_{70} in our case)[20] are involved. Moreover, few papers in literature report a detailed comparison between model output and experimental data (especially concerning the responses to the variation in operating conditions) when a mechanistic model is applied to the hydrocracking of long chain paraffins or complex feedstocks.

For these reasons, in the present research, a molecular-level model of the pathway type, i.e., including only observable molecules and not intermediates, has been chosen instead of a mechanistic one.[19] Since a vapor−liquid equilibrium calculation is performed by means of the SRK EoS at each integration step (vapor−liquid equilibrium plus reaction model),[20] the kinetic equations can be usefully written in terms of fugacities:[33]

$$\frac{dY_{iso\text{-}C}(i)}{d\tau} = r_{isom}(i) + r_{prod,iso\text{-}C}(i) - r_{cr}(i) \quad i = 6, 70 \tag{3}$$

$$\frac{dY_{iso\text{-}C}(i)}{d\tau} = r_{isom}(i) + r_{prod,iso\text{-}C}(i) \quad i = 5 \tag{4}$$

$$\frac{dY_{iso\text{-}C}(i)}{d\tau} = r_{prod,iso\text{-}C}(i) \quad i = 4 \tag{5}$$

$$\frac{dY_{n\text{-}C}(i)}{d\tau} = -r_{isom}(i) + r_{prod,n\text{-}C}(i) \quad i = 6, 70 \tag{6}$$

$$\frac{dY_{n\text{-}C}(i)}{d\tau} = -r_{isom}(i) + r_{prod,n\text{-}C}(i) + 2/5 r_{cr}(i+1) \quad i = 5 \tag{7}$$

$$\frac{dY_{n\text{-}C}(i)}{d\tau} = r_{prod,n\text{-}C}(i) + 2/5 r_{cr}(i+2) \quad i = 4 \tag{8}$$

$$\frac{dY_{n\text{-}C}(i)}{d\tau} = r_{prod,n\text{-}C}(i) + 2/5 r_{cr}(i+3) \quad i = 3 \tag{9}$$

$$\frac{dY_{n\text{-}C}(i)}{d\tau} = 2/5 r_{cr}(i+4) \quad i = 2 \tag{10}$$

$$\frac{dY_{n\text{-}C}(i)}{d\tau} = 2/5 r_{cr}(i+5) \quad i = 1 \tag{11}$$

where

$$r_{prod,iso\text{-}C}(i) = \gamma \sum_{j=i+4}^{70} \left[\frac{2}{j-6} r_{cr}(j)\right] + \frac{1}{(i+3)-6} r_{cr}(i+3) \quad i = 4, 66 \tag{12}$$

$$r_{prod,iso\text{-}C}(i) = \frac{1}{(i+3)-6} r_{cr}(i+3) \quad i = 67 \tag{13}$$

$$r_{prod,n\text{-}C}(i) = (1-\gamma) \sum_{j=i+4}^{70} \left[\frac{2}{j-6} r_{cr}(j)\right] \quad i = 4, 66 \tag{14}$$

$$r_{prod,n\text{-}C}(i) = \sum_{j=7}^{70} \left[\frac{1}{j-6} r_{cr}(j)\right] \quad i = 3 \tag{15}$$

$$r_{isom}(i) = \frac{k^0_{isom}(i) e^{-E_{isom}(i)/(RT)}}{ADS} (fug_{n\text{-}C}(i) - fug_{iso\text{-}C}(i)/K_{eq}(i)) \tag{16}$$

$$r_{cr}(i) = \frac{k^0_{cr}(i) e^{-E_{cr}(i)/(RT)} fug_{iso\text{-}C}(i)}{ADS} \tag{17}$$

$$ADS = fug_{H_2}[1 + \sum_{i=1}^{70} K_{L_{n\text{-}C}}(i) fug_{n\text{-}C}(i) + \sum_{i=4}^{70} K_{L_{iso\text{-}C}}(i) fug_{iso\text{-}C}(i)] \tag{18}$$

A condition of thermodynamic equilibrium between the phases is justified because experimental tests were carried out in a bench scale reactor with a powdered catalyst, i.e., the size of the catalyst powder was chosen so as to ensure that inter- and intraphase resistances were negligible.

Equations 3−11 are able to simulate the behavior of an isothermal plug flow reactor without axial or radial diffusion; which is in accordance with the experimental apparatus, a bench scale trickle bed reactor operated in down flow mode.[20]

Since the same kinetic expression has been used for both vapor and liquid, the equations for the two phases can be summed up so that a unique balance equation is obtained. This can also be correctly done applying a different multiplying factor to the reaction term for liquid and vapor (higher reactivity of liquid phase has been observed by Calemma et al.).[8] This is due to the type of dependent and independent variables in the model, coherent with the variables used for experimental data, which represent the global system behavior without differentiating between liquid and vapor phases:

$$\tau = \left[\frac{kg_{cat}\cdot h}{kg_{n\text{-}C_{in}}}\right] \tag{19}$$

$$Y = \left[\frac{kmol}{kg_{n\text{-}C_{in}}}\right] \tag{20}$$

The present model represents the most advanced result of an investigation started considering a lumped model[34] where hydrocarbons were grouped into pseudocomponents correspond-

ing to merceological requirements. The simplifying hypotheses have been removed one by one, and, in particular, the behavior of each hydrocarbon can be described, with the exception of isomers (a generic class of branched paraffins is considered for each number of carbon atoms) because detailed experimental evidence on isomer distribution for high n_C are unfeasible.[35] The assumption of the vapor phase alone inside the reactor has been removed[20,33,36] as well as, in this paper, the one that isoalkanes break in the middle of the chain (this simplifying hypothesis has been recently used for modeling purposes by other authors as well).[37]

The correlations used for the kinetic constants are the following where the parameters are obtained by a nonlinear regression program based on the least-squares method:

$$K_{L_{n\text{-}C}}(i) = 83.51e^{[-\Delta H_{ads,n\text{-}C}(i)/\langle RT\rangle]} \quad (21)$$

$$\frac{\Delta H_{ads,n\text{-}C}(i)}{R} = -(79.00 + 280.77i) \quad (22)$$

$$K_{L_{iso\text{-}C}}(i) = 64.13e^{[-\Delta H_{ads,iso\text{-}C}(i)/\langle RT\rangle]} \quad (23)$$

$$\frac{\Delta H_{ads,iso\text{-}C}(i)}{R} = -(0.03 + 261.97i) \quad (24)$$

$$k^0_{cr}(i) = 1.95 \times 10^{15} i^{7.56} \quad (25)$$

$$E_{cr}(i) = 2.28 \times 10^4 \ln(i) + 7.15 \times 10^4 \quad (26)$$

$$K_{eq}(i) = [0.13e^{(0.31i)}]e^{\{-\Delta H_{isom}/R[\langle 1/T\rangle - \langle 1/632.15\rangle]\}} \quad (27)$$

$$k^0_{isom}(i) = 3.74 \times 10^{16} i^{7.65} \quad (28)$$

$$E_{isom}(i) = 1.41 \times 10^4 \ln(i) + 1.04 \times 10^5 \quad (29)$$

The expressions of the Langmuir and equilibrium constants have been modified taking into account the dependence on temperature.

The adsorption of the paraffins on the type of catalyst used for this study is a very strong physical adsorption (always exothermic).

The ΔH_{ads} has been expressed as a linear function of the paraffins' carbon number. In such a way, for a given temperature, Langmuir constants remain an exponential function of the carbon number.[20,35]

As for the equilibrium constants, the dependence on temperature has been introduced. The exponential form as well as the values of ΔH_{isom} have been derived in a previous thermodynamic study.[38]

The analysis of the values obtained for the kinetic constants from eqs 21−29 brings to the following conclusions: (a) The Langmuir constants, at the same n_C value, increase with a decreasing temperature, according to the exothermic physical adsorption. The $K_{L_{iso\text{-}C}}$ are, as expected, lower than the $K_{L_{n\text{-}C}}$. (b) For the heavy paraffins (n-C_{22+}), regardless of temperature, the high K_{eq} value shows an equilibrium heavily shifted to the right. (c) The heats of adsorption for n-paraffins range from −2.99 kJ/mol (C_1) to −164.06 kJ/mol (C_{70}), while for iso-paraffins they range from −8.71 kJ/mol (C_4) to −152.46 kJ/mol (C_{70}). Thus the adsorption of lightest paraffins is correctly negligible. (d) The activation energies of the isomerization reaction range from 126.69 kJ/mol (C_5) to 163.90 kJ/mol (C_{70}). (e) The activation energies of the cracking reaction range from 112.35 kJ/mol (C_6) to 168.37 kJ/mol (C_{70}).

Both the heats of adsorption and the activation energies show acceptable order of magnitude. Moreover, there is not an important change in the values of the activation energies with the number of carbon atoms, and for the same paraffin (especially at high n_C), there is not a significant difference between the activation energy for isomerization and for cracking according to what was stated by Martens et al.[18]

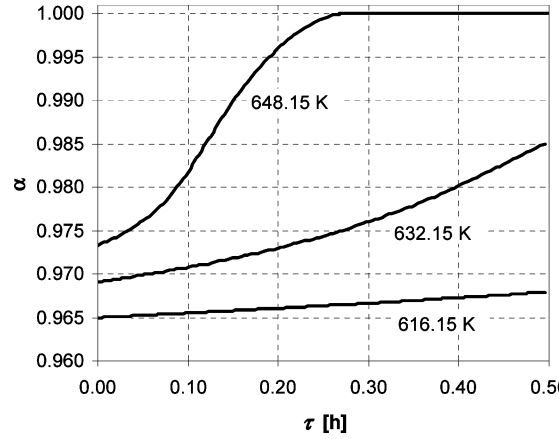

Figure 1. Molar vapor fraction profile along the reactor.

5. Numerical Problems and Their Solution

As has already been noted,[20,34] the model does not present problems of stiffness, and therefore, the equations have been solved using a Runge−Kutta method of fourth-order with constant step. The error in the carbon balance due to the approximations of the integrating functions is equal to 5.2×10^{-6}%.

Numerical problems connected to the model are due to the discontinuity rising for high conversions at the transition from the vapor−liquid equilibrium (VLE) state to the vapor phase alone. Moreover, in the meantime, composition changes for the reaction. Figure 1 shows molar vaporization ratio profiles along the reactor for three test runs characterized by the same values of pressure and H_2/waxes mass ratio, but different temperatures.

Since while the reaction proceeds the stream becomes lighter because of cracking, the molar vapor fraction increases along the reactor. In particular for the test characterized by the highest temperature of the whole experimental plan, α reaches the value of 1 in proximity to the middle of the reactor for both kinetic and thermodynamic factors.

The small discontinuities due to this transition are greatly amplified by the denominator of the kinetic equations where fugacities are multiplied by Langmuir constants whose values vary (at 632.15 K), in order of magnitude, from 10^2 to 10^{15} 1/Pa. To avoid these numerical instabilities, the integration step has been reduced at the boundary between vapor−liquid equilibrium (VLE) and vapor phase. Then, the step has been increased again.

Another numerical problem has been detected at high conversions when n-paraffins have almost completely disappeared, i.e., when the Y values for n-paraffins reach values of the order of magnitude (in double precision) of 10^{-9} (that corresponds to molar fractions of the order of 10^{-7}−10^{-6}). In this case, the isomerization equilibrium gives rise to oscillations between n-paraffins and iso-paraffins, i.e., to numerical instability. To solve such a problem, we have adopted the following method: for Y of the heavy n-paraffins below 5.0×10^{-9}, the corresponding r_{isom} has been deleted and the products with the same n_C coming from cracking of higher paraffins have been considered completely branched.

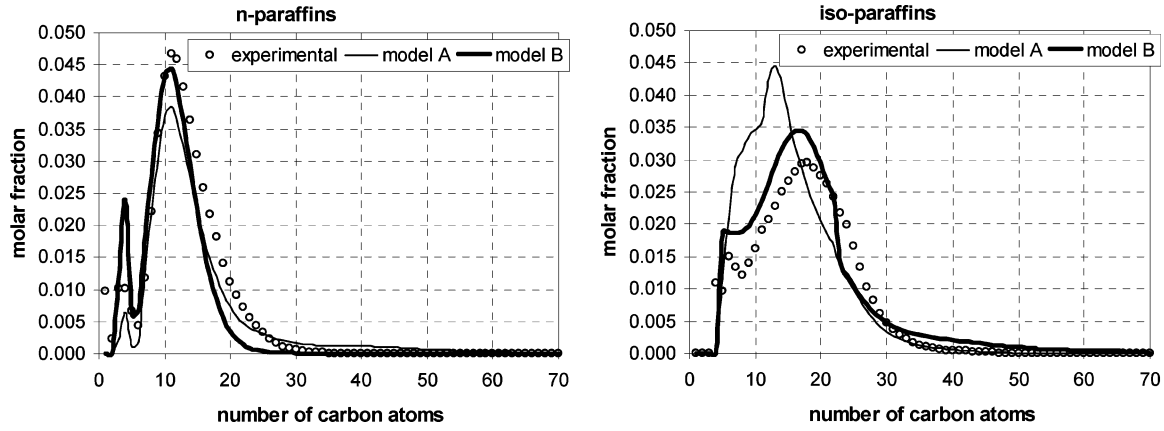

Figure 2. Results for the test run with temperature 632.15 K; pressure 47.5 bar; H_2/waxes 0.1050 kg/kg; WHSV 2 1/h (central test in the experimental plan).[20,21] (model A) Model with breakage in the middle. (model B) Model with breakage probability function.

6. Results and Discussion

In the following figures, the molar fractions of the products vs the number of carbon atoms are reported for some tests, compared with the results from the model with breakage in the middle[20] and with experimental values. The analyzed tests regard the two situations of variable temperature with the other operating conditions kept constant (Figures 2 and 3) and of variable H_2/waxes mass ratio (Figures 2 and 4), these two being the most significant parameters.

It is evident that the introduction of the breakage probability function improves the estimate of the product distribution especially for iso-paraffins. In particular the calculated product distributions are closer to the experimental ones in the C_5-C_{14} range, assuring a better prediction of the isomer percentage in gasoline and kerosene cuts. Also the prediction of the C_1-C_4 products is generally better than that of the previous model even if methane and ethane are underestimated.

The analysis of the global variables characterizing the system (mass conversion, MD percentage, and isomer percentage) shows that they are in accordance with the experimental data (Figures 5−7).

The conversion refers to the waxes (C_{22+}) and it is defined as follows:

$$\xi_{C_{22+}} = \frac{\omega_{C_{22+in}} - \omega_{C_{22+out}}}{\omega_{C_{22+in}}} \times 100 \qquad (30)$$

The MD percentage in the product stream is defined as follows:

$$\%\mathrm{MD} = 100(\omega_{\mathrm{totalC_{10}-C_{14out}}} + \omega_{\mathrm{totalC_{15}-C_{22out}}}) \qquad (31)$$

The isomer percentage in the product stream is defined as follows:

$$\%\text{iso-C} = 100 \sum_{i=4}^{70} \omega_{\text{iso-C}_{out}}(i) \qquad (32)$$

The influence of the variables of interest on the weight fractions of the outlet lumps is shown by Figures 8−11.

The figures show that the model gives correct responses to the changes in T, P, H_2/waxes mass ratio, and WHSV: the values computed by the model are close to the experimental ones.

From the trend of lump C_{22+}, it is possible to derive the effect of each variable on the conversion: (a) conversion increases with temperature. This means that between the two opposite effects, i.e., the decrease of K_L (adsorption of *n*-paraffins is more difficult) and the increase in the rate of reaction, it is the latter to prevail. The two opposite effects make the influence of temperature on conversion not so strong at the borders of the experimental field (in terms of temperature); (b) conversion decreases with pressure. By increasing pressure, the fugacity of hydrogen increases affecting negatively the dehydrogenation equilibrium of feed paraffins and, consequently, the total conversion; (c) conversion increases with the H_2/waxes mass ratio;[20] (d) an increased space velocity means a decreased contact time and, consequently, a decreased conversion.

In order to complete the analysis of the model, the diagrams of Y vs τ have been reported for a given test run, characterized by the lowest space velocity of the experimental plan (Figure 12).

It has to be pointed out that the analysis of the reactor profiles has been useful to detect and solve the numerical problems previously described.

From the analysis of the profiles along the reactor, it can be pointed out that (a) the lump C_{22+}, after an initial phase at nearly constant concentration (where isomerization is controlling, since the isomer concentration is too low to allow cracking to take place significantly), quickly disappears until its concentration is of 1 order of magnitude lower than in the feed; (b) lumps iso-C_5-C_9, iso-$C_{10}-C_{14}$, and iso-$C_{15}-C_{22}$ increase their concentration along the reactor, since the isomerization rate of the corresponding *n*-lump (increasing with n_C) and the production rate from the heavier lumps are more significant than the rate of cracking; (c) lumps C_1-C_4 and *n*-C_5-C_9, that are almost unaffected by isomerization (iso-butane is formed only from cracking of heavier hydrocarbons), increase their concentration due to production from heavier hydrocarbons; (d) for lumps *n*-$C_{10}-C_{14}$ and *n*-$C_{15}-C_{22}$, the isomerization rate (that increases with n_C) is higher than the production rate from the heavier hydrocarbons, and therefore, such lumps are consumed as the reaction goes on.

7. Conclusions

A model of the trickle-bed reactor, without inter- and intraphase resistances, for the hydrocracking of the FT waxes has been worked out. For its development, both kinetic and thermodynamic factors have been taken into account. In regards to kinetics, a pathway-level scheme, based on the Langmuir−Hinshelwood−Hougen−Watson mechanism, with a proper breakage probability for the C−C bonds, has been built. This breakage probability function (quite simple but reliable) has been derived from literature works on model

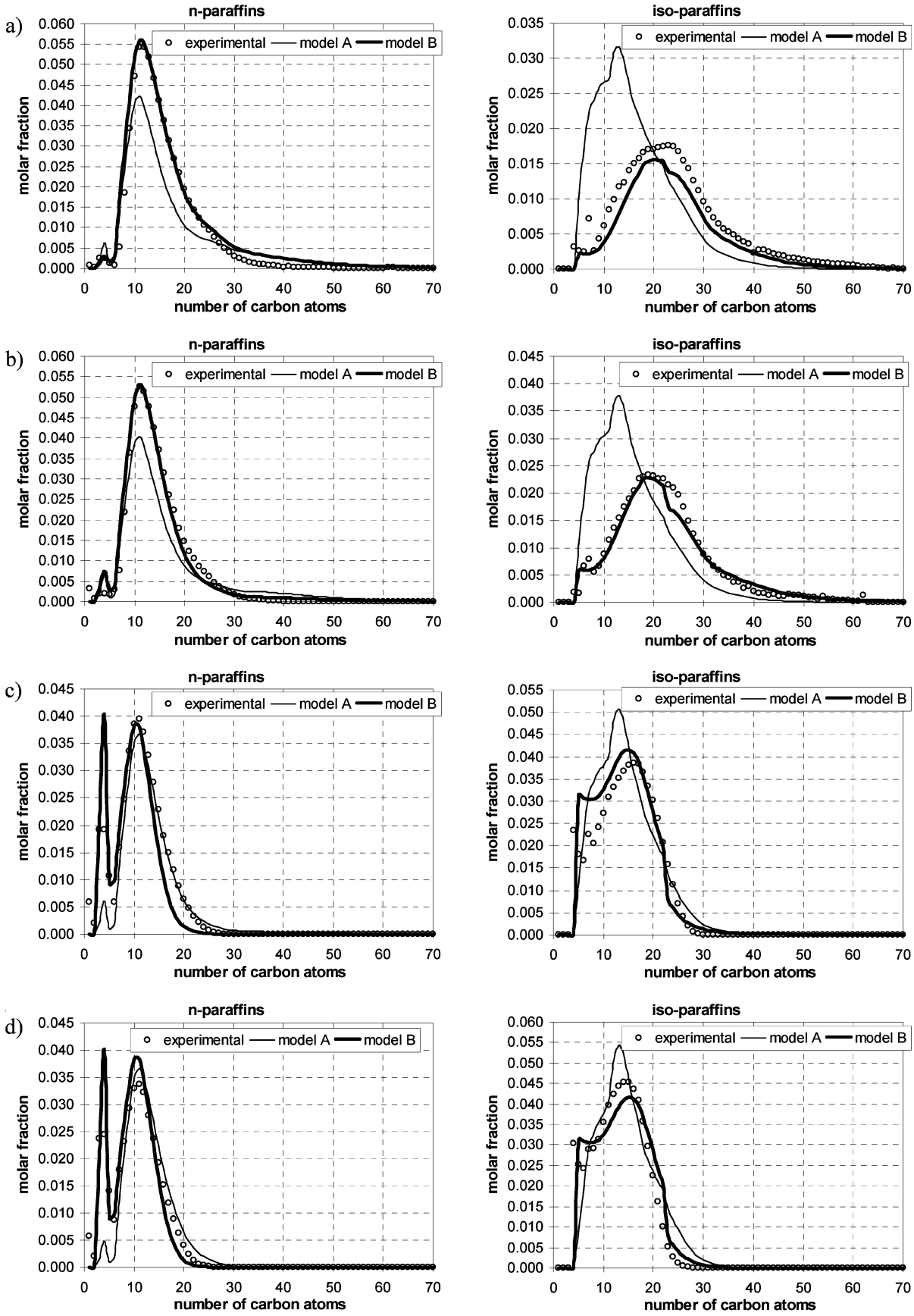

Figure 3. Results for the test runs with pressure 47.5 bar; H_2/waxes 0.1050 kg/kg; WHSV 2 1/h and different temperatures: (a) 616.15; (b) 624.15; (c) 640.15; (d) 648.15 K. (model A) Model with breakage in the middle. (model B) Model with breakage probability function.

compounds. From a thermodynamic standpoint, in addition to the VLE calculation already included in the reactor model, to correctly account for the H_2/waxes mass ratio effect,[20] temperature and carbon atom number depending functions for Langmuir constants for physical adsorption, and equilibrium constants for isomerization reactions, have been

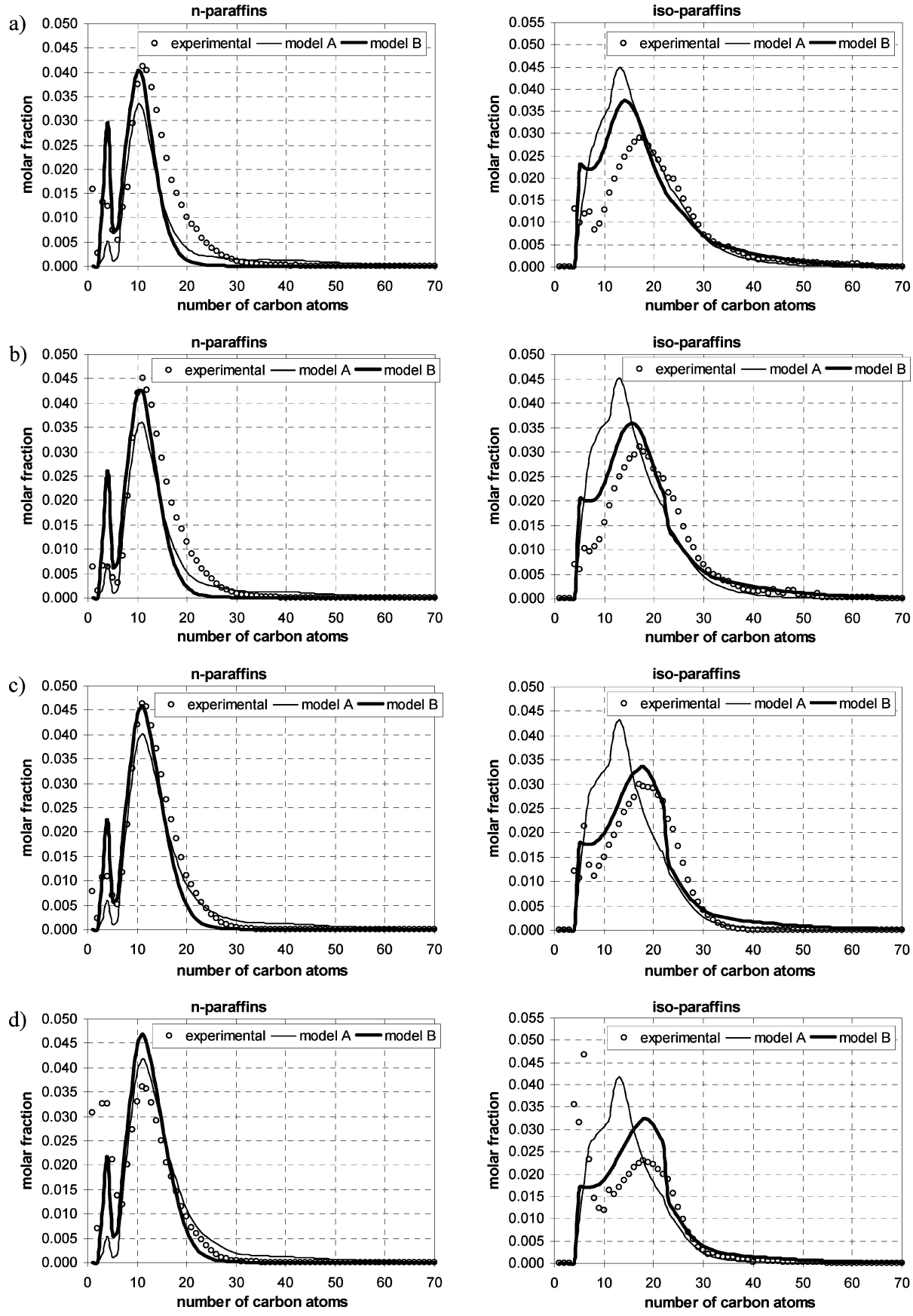

Figure 4. Results for the test runs with temperature 632.15 K; pressure 47.5 bar; WHSV 2 1/h and different H_2/waxes ratios: (a) 0.0600; (b) 0.0825; (c) 0.1275; (d) 0.1500 kg/kg. (model A) Model with breakage in the middle. (model B) Model with breakage probability function.

developed. The details about the thermodynamic study have been reported elsewhere.[20,36,38]

The results show a clear improvement over the previous models.[20,34,35] In particular, the introduction of the breakage

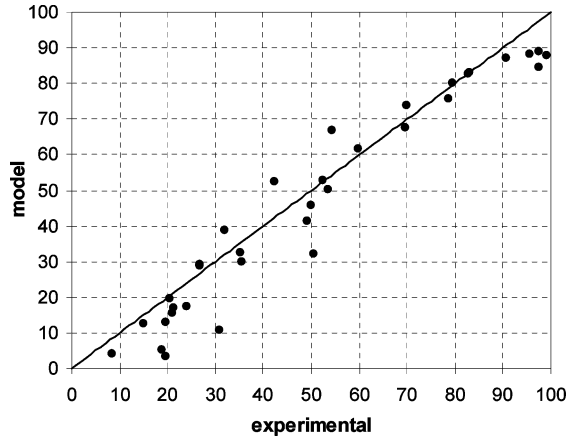

Figure 5. Parity plot of conversion.

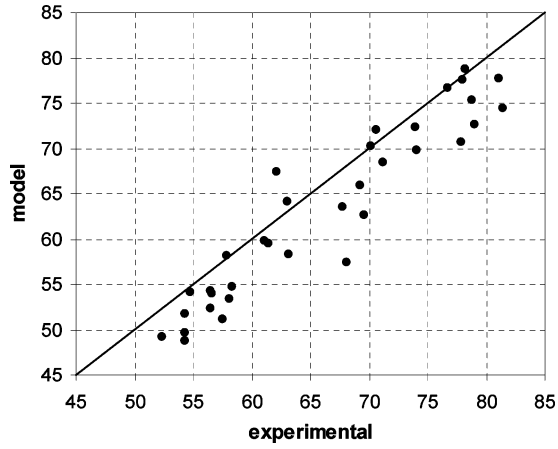

Figure 6. Parity plot of MD percentage.

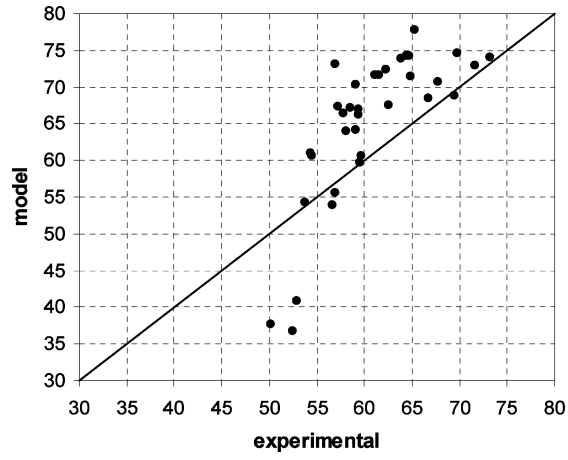

Figure 7. Parity plot of isomer percentage.

probability function, together with new functions for equilibrium constants of isomerization reactions, has enhanced the agreement between calculated and experimental product distributions especially for iso-paraffins. Furthermore, the assumption of the dependence on temperature of the Langmuir constants allows the model to accurately account for the temperature's effect (that is both a thermodynamic and a kinetic effect) on conversion at the extremities of the experimental field.

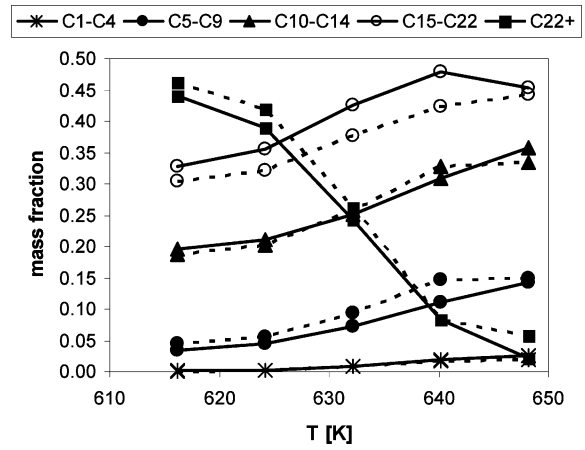

Figure 8. Temperature effect on the outlet lumps (pressure 47.5 bar; H_2/waxes 0.1050 kg/kg; WHSV 2 1/h); (continuous lines) experimental; (dotted lines) calculated.

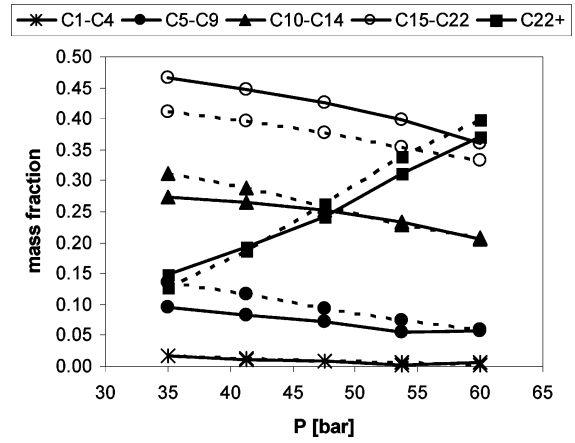

Figure 9. Pressure effect on the outlet lumps (temperature 632.15 K; H_2/waxes 0.1050 kg/kg; WHSV 2 1/h); (continuous lines) experimental; (dotted lines) calculated.

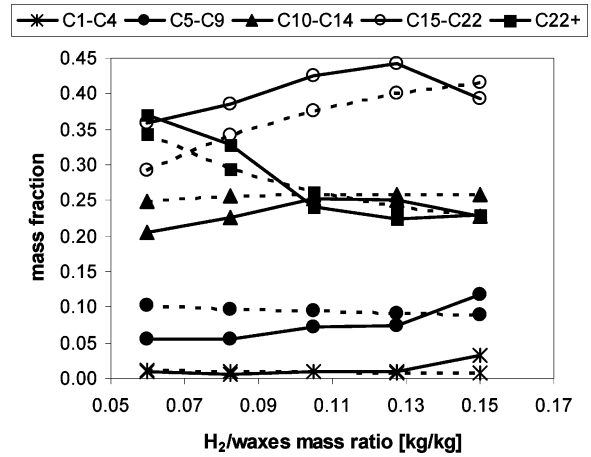

Figure 10. Hydrogen to waxes mass ratio effect on the outlet lumps (temperature 632.15 K; pressure 47.5 bar; WHSV 2 1/h); (continuous lines) experimental; (dotted lines) calculated.

Globally, the model provides a better fit of experimental data for the operating conditions corresponding to low and high conversion.

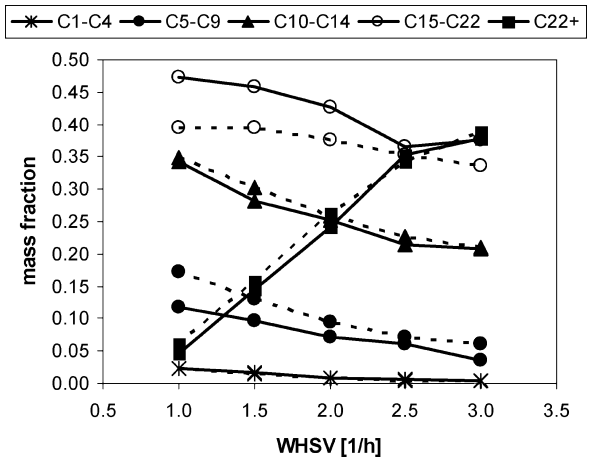

Figure 11. WHSV effect on the outlet lumps (temperature 632.15 K; pressure 47.5 bar; H_2/waxes 0.1050 kg/kg): (continuous lines) experimental; (dotted lines) calculated.

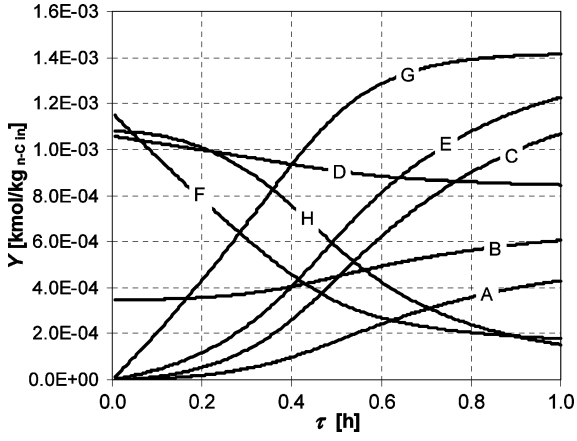

Figure 12. Lumps profiles along the reactor. (A) total C_1-C_4; (B) n-C_5-C_9; (C) iso-C_5-C_9; (D) n-$C_{10}-C_{14}$; (E) iso-$C_{10}-C_{14}$; (F) n-$C_{15}-C_{22}$; (G) iso-$C_{15}-C_{22}$; (H) total C_{22+}.

Thus, correctly accounting for both thermodynamic and kinetic effects, reliable results can be obtained in modeling the hydrocracking of a complex feedstock (n-C_5-C_{70} mixture), as shown by the reported parity plots for global variables (mass conversion, MD percentage, and isomer percentage), as well as by the model responses to the variation of the operating conditions.

Nomenclature

ΔH_{ads} = variation of enthalpy associated with physical adsorption (kJ/kmol)
ΔH_{isom} = variation of enthalpy associated with isomerization reactions (kJ/kmol)
E = activation energy (kJ/kmol)
fug = fugacity (Pa)
i = number of carbon atoms
j = number of carbon atoms
k^0 = frequency factor (kmol/(kg_{cat}·h))
K_{eq} = equilibrium constant of isomerization
K_L = Langmuir constant for physical adsorption (1/Pa)
MW = molecular weight
n_C = number of carbon atoms
r = reaction rate (kmol/(kg_{cat}·h))
R = universal gas constant (kJ/(kmol·K))
T = temperature (K)
Y = moles to inlet waxes mass ratio (kmol/$kg_{n\text{-}C_{in}}$)

Greek Symbols

α = molar vapor fraction
γ = fraction of branched paraffins coming from cracking of heavier hydrocarbons
ξ = conversion
τ = contact time (kg_{cat}·h/$kg_{n\text{-}C_{in}}$)
ω = mass fraction

Subscripts

cat = catalyst
cr = relevant to cracking reactions
H_2 = hydrogen
in = inlet
iso-C = relevant to branched paraffins
isom = relevant to isomerization reactions
n-C = relevant to n-paraffins
out = outlet
prod = production by cracking of heavier hydrocarbons

Literature Cited

(1) Dry, M. E. The Fischer−Tropsch Process: 1950−2000. *Catal. Today* **2002**, *71*, 227.

(2) Sie, S. T.; Senden, M. M. G.; Van Wechem, H. M. H. Conversion of Natural Gas to Transportation Fuels via the Shell Middle Distillate Synthesis Process (SMDS). *Catal. Today* **1991**, *8*, 371.

(3) Leckel, D.; Liwanga-Ehumbu, M. Diesel-Selective Hydrocracking of an Iron-Based Fischer−Tropsch Wax Fraction ($C_{15}-C_{45}$) Using a MoO_3-Modified Noble Metal Catalyst. *Energy Fuels* **2006**, *20*, 2330.

(4) Dancuart, L. P.; de Haan, R.; de Klerk, A. Processing of Primary Fischer−Tropsch Products. In *Fischer−Tropsch Technology*; Steynberg, A., Dry, M., Eds.; Studies in Surface Science and Catalysis; Elsevier: Amsterdam; 2004; Vol. 152, p 482.

(5) Weitkamp, J.; Ernst, S. Factors Influencing the Selectivity of Hydrocracking in Zeolites. In *Guidelines for Mastering the Properties of Molecular Sieves*; Barthomeuf, D., Derouane, E. D., Holderich, W., Eds.; Plenum Press: New York, 1990; p 343.

(6) Archibald, R. C.; Greensfelder, B. S.; Holzman, G.; Rowe, D. H. Catalytic Hydrocracking of Aliphatic Hydrocarbons. *Ind. Eng. Chem.* **1960**, *52*, 745.

(7) Gibson, J. W.; Good, G. M.; Holzman, G. The Use of Dual Function Catalysts in Isomerization of High Molecular Weight n-Paraffins. *Ind. Eng. Chem.* **1960**, *52*, 113.

(8) Calemma, V.; Peratello, S.; Pavoni, S.; Clerici, G.; Perego, C. Hydroconversion of a Mixture of Long Chain n-Paraffins to Middle Distillate: Effect of the Operating Parameters and Products Properties. In *Natural Gas Conversion VI*; Iglesia, E., Spivey, J. J., Fleish, T. H., Eds.; Studies in Surface Science and Catalysis; Elsevier: Amsterdam; 2001; Vol. 136, p 307.

(9) Calemma, V.; Guanziroli, S.; Pavoni, S.; Giardino, R. *Process for the Production of Paraffinic Middle Distillates*. European Patent EP1404783 (B1), 2005.

(10) Kaufmann, T. G.; Kaldor, A.; Stuntz, G. F.; Kerby, M. C.; Ansell, L. L. Catalysis Science and Technology for Cleaner Transportation Fuels. *Catal. Today* **2000**, *62*, 77.

(11) Collins, J. P.; Font Freide, J. J. H. M.; Nay, B. A History of Fischer−Tropsch Wax Upgrading at BP—From Catalyst Screening Studies to Full Scale Demonstration in Alaska. *J. Nat. Gas Chem.* **2006**, *15*, 1.

(12) O'Rear, D. J. *Distillate Fuel Blends from Fischer Tropsch Products with Improved Seal Swell Properties*. United States Patent 6,890,423, 2005.

(13) Euzen, P.; Gueret, C. *Method for Producing Middle Distillates by the Hydroisomerization and Hydrocracking of Feedstocks Obtained from the Fischer−Tropsch Method*. European Patent EP1893724 (A1), 2008.

(14) Akhmedov, V. M.; Al-Khowaiter, S. H. Recent Advances and Future Aspects in the Selective Isomerization of High n-Alkanes. *Cat. Rev.−Sci. Eng.* **2007**, *49*, 33.

(15) Schulz, H. F.; Weitkamp, J. H. Zeolite Catalysts. Hydrocracking and Hydroisomerization of n-Dodecane. *Ind. Eng. Chem. Prod. Res. Dev.* **1972**, *11*, 46.

(16) Steijns, M.; Froment, G.; Jacobs, P.; Uytterhoeven, J.; Weitkamp, J. Hydroisomerization and Hydrocracking. 2. Product Distributions from n-Decane and n-Dodecane. *Ind. Eng. Chem. Prod. Res. Dev.* **1981**, *20*, 654.

(17) Weitkamp, J. Isomerization of Long-Chain n-Alkanes on a Pt/CaY Zeolite Catalyst. *Ind. Eng. Chem. Prod. Res. Dev.* **1982**, *21*, 550.

(18) Martens, J. A.; Jacobs, P. A.; Weitkamp, J. Attempts to Rationalize the Distribution of Hydrocracked Products. I. Qualitative Description of the Primary Hydrocracking Modes of Long Chain Paraffins in Open Zeolites. *Appl. Catal* **1986**, *20*, 239.

(19) Klein, M. T.; Hou, G. Mechanistic Kinetic Modeling of Heavy Paraffin Hydrocracking. In *Practical Advances in Petroleum Processing*; Hsu, C. S., Robinson, P. R., Eds.; Springer Science and Business Media, Inc: New York, 2006; Vol. 2; p 187.

(20) Pellegrini, L. A.; Gamba, S.; Calemma, V.; Bonomi, S. Modelling of Hydrocracking with Vapour−Liquid Equilibrium. *Chem. Eng. Sci.* **2008**, *63*, 4285.

(21) Calemma, V.; Correra, S.; Perego, C.; Pollesel, P.; Pellegrini, L. Hydroconversion of Fischer−Tropsch Waxes: Assessment of the Operating Conditions Effect by Factorial Design Experiments. *Catal. Today* **2005**, *106*, 282.

(22) Egloff, G.; Morrell, J. C.; Thomas, C. L.; Bloch, H. S. The Catalytic Cracking of Aliphatic Hydrocarbons. *J. Am. Chem. Soc.* **1939**, *61*, 3571.

(23) Haensel, V. Catalytic Cracking of Pure Hydrocarbons. In *Advances in Catalysis and Related Subjects*; Frankenburg, W. G., Eds.; Academic Press, Inc: New York, 1951; Vol. III, p 179.

(24) Sie, S. T. Acid-Catalyzed Cracking of Paraffinic Hydrocarbons. 1. Discussion of Existing Mechanisms and Proposal of a New Mechanism. *Ind. Eng. Chem. Res.* **1992**, *31*, 1881.

(25) Sie, S. T. Acid-Catalyzed Cracking of Paraffinic Hydrocarbons. 3. Evidence for the Protonated Cyclopropane Mechanism from Hydrocracking/Hydroisomerization Experiments. *Ind. Eng. Chem. Res.* **1993**, *32*, 403.

(26) Haag, W. C.; Dessau, R. M. Duality of Mechanism in Acid-Catalyzed Paraffin Cracking. In *Proceedings of the 8th Congress on Catalysis*; Verlag Chemie: Weinheim, 1984; Vol. II, p II-305.

(27) Weitkamp, J. The Influence of Chain Length in Hydrocracking and Hydroisomerization of n-Alkanes. In *Hydrocracking and Hydrotreating*; Ward, J. W., Qader, S. A., Eds.; ACS Symposium Series 20; American Chemical Society: Washington, DC, 1975; p 1.

(28) Weitkamp, J. Hydrocracking, Cracking and Isomerization of Hydrocarbons. *Erdoel, Kohle, Erdgas, Petrochem.* **1978**, *31*, 13.

(29) Coonradt, H. L.; Garwood, W. E. Mechanism of Hydrocracking. Reactions of Paraffins and Olefins. *Ind. Eng. Chem. Proc. Des. Dev.* **1964**, *3*, 38.

(30) Langlois, G. E.; Sullivan, R. F.; Egan, C. J. The Effect of Sulfiding a Nickel on Silica-Alumina Catalyst. *J. Phys. Chem.* **1966**, *70*, 3666.

(31) Langlois, G. E.; Sullivan, R. F. Chemistry of Hydrocracking. In *Refining Petroleum for Chemicals*; Spillane, L. J., Leftin, H. P., Eds.; Advances in Chemistry Series 97; American Chemical Society: Washington, DC, 1970; p 38.

(32) Sie, S. T.; Eilers, J.; Minderhoud, J. K. Consequences of Fischer-Tropsch Chain Growth Kinetics for Process Mode Selection and Product Selectivity. In *Proceedings of the 9th International Congress on Catalysis*; Phillips, M. J., Ternan, M., Eds.; The Chemical Institute of Canada: Ottawa, 1988; Vol. 2, p 743.

(33) Pellegrini, L.; Gamba, S.; Calemma, V.; Bonomi, S. Hydrocracking Reactor Model with Vapor/Liquid Equilibrium. In *2007 AIChE Annual Meeting Conference Proceedings*, AIChE Annual Meeting, Salt Lake City, UT, Nov 4−9, 2007; AIChE: New York, 2007; paper 427g.

(34) Pellegrini, L.; Locatelli, S.; Rasella, S.; Bonomi, S.; Calemma, V. Modeling of Fischer−Tropsch Products Hydrocracking. *Chem. Eng. Sci.* **2004**, *59*, 4781.

(35) Pellegrini, L.; Bonomi, S.; Gamba, S.; Calemma, V.; Molinari, D. The "All Components Hydrocracking Model". *Chem. Eng. Sci.* **2007**, *62*, 5013.

(36) Gamba, S.; Soave, G. S.; Pellegrini, L. A. Use of Normal Boiling Point Correlations for Predicting Critical Parameters of Paraffins for Vapour−Liquid Equilibrium Calculations with the SRK Equation of State. *Fluid Phase Equilib.* **2009**, *276*, 133.

(37) Fernandes, F. A. N.; Teles, U. M. Modeling and Optimization of Fischer−Tropsch Products Hydrocracking. *Fuel Process. Technol.* **2007**, *88*, 207.

(38) Pellegrini, L. A.; Gamba, S.; Bonomi, S.; Calemma, V. Equilibrium Constants for Isomerization of n-Paraffins. *Ind. Eng. Chem. Res.* **2007**, *46*, 5446.

Received for review December 17, 2008
Revised manuscript received April 3, 2009
Accepted April 14, 2009

IE8019455